Am J Cancer Res 2026;16(1):125-140
www.ajcr.us /ISSN:2156-6976/ajcr0165808

Original Article

PRMT5 inhibits the ferroptosis of hepatocellular carcinoma via regulating RBM15/FTH1 signaling

Jiayu Chen*, Xinyao Hu*, Yang Shen*, Yukai Chen, Le Xu, Ling Wang, Ximing Xu

*Cancer Center, Renmin Hospital of Wuhan University, Wuhan 430060, Hubei, China. *Equal contributors.*

Received May 4, 2025; Accepted October 23, 2025; Epub January 15, 2026; Published January 30, 2026

Abstract: Hepatocellular carcinoma (HCC) is one of the most malignant tumors worldwide. This study aimed to investigate the role of protein arginine methyltransferase 5 (PRMT5) in HCC. Gene expression was determined using reverse transcription-quantitative polymerase chain reaction, Western blot, and immunohistochemistry. The interaction between genes were determined using chromatin immunoprecipitation, glutathione-S-transferase pull-down, co-immunoprecipitation, and luciferase assays. m6A levels were determined using m6A dot assay. N6-methyladenosine (m6A) enrichment was determined using methylated RNA immunoprecipitation assay. Cellular functions were determined using Cell Counting Kit-8 assay and propidium iodide staining. Xenograft assay was conducted to further verify the role of PRMT5 in HCC. We found that overexpressed PRMT5 was upregulated in tumor protein p53 (TP53)-mutated HCC patients. TP53 epigenetically in activated PRMT5. PRMT5 deficiency promoted the ferroptosis of HCC cells *in vitro* and inhibited tumor growth *in vivo*. Moreover, PRMT5 could interact with RNA binding motif protein 15 (RBM15) to activate ferritinophagy signaling. RBM15-mediated m6A modification of ferritin heavy chain 1 (FTH1), promoting its mRNA expression and stability. However, overexpression of FTH1 suppressed ferroptosis and promoted tumor growth. Taken together, PRMT5/RBM15/ferritinophagy signaling can be a potential target for HCC.

Keywords: Hepatocellular carcinoma, protein arginine methyltransferase 5, ferroptosis, N6-methyladenosine modification

Introduction

Hepatocellular carcinoma (HCC) is characterized with high morbidity and mortality [1]. In China, HCC ranks as the second dangerous malignancy and nearly 400,000 cases are HCC-related death [2]. Although marked advances have been made in the treatment of HCC, the long-term survival rate of HCC patients are still poor [3, 4]. Postoperative recurrence and metastasis are the key causes of HCC-related death [5]. Thence, to explore the potential mechanisms is of vital importance.

Ferroptosis is form of cell death featured by oxidative stress, lipid peroxidation, and iron accumulation [6]. However, cells evolve the following three mechanisms to protect cells from ferroptotic death: glutathione (GSH), coenzyme Q10, and thioredoxin systems [7]. Ferritinophagy is regulated by autophagic cargo receptor nuclear receptor coactivator 4 (NCOA4) and iron storage protein complex, such as ferritin heavy chain 1 (FTH1) and ferritin light chain (FTL) [8]. NCOA4 directly binds to FTH1 and drives the ferritins to autophagosomes for lysosomal degradation and iron release, resulting in ferroptosis-related cell death [9]. Recently, targeting ferroptosis signaling is a potential strategy for HCC. Activation of ferritinophagy alleviates sorafenib resistance in HCC [10]. Therefore, targeting ferritinophagy may be a potential strategy for stimulating the ferroptosis of HCC.

Arginine methylation is a common form of post-translational modifications (PTMs) and regulated by protein arginine methyltransferases (PRMTs) [11]. PRMTs can be categorified into the following three types: monomethylarginine, symmetric dimethylarginine, as well as asymmetric dimethylarginine [12]. The abnormal levels of arginine methylation or PRMTs are involved in carcinogenesis, including HCC [13]. PRMT5, a member of type II enzymes, promotes the proliferation and development of HCC [14]. Intriguingly, targeting PRMT5 with its spe-

cific inhibitor GSK3326595 evokes anti-tumor immunity and suppresses tumor growth [15]. However, the underlying mechanism is still unknown.

The present study investigated the potentials of PRMT5 in HCC. Overexpressed PRMT5 predicted poor clinical outcomes of HCC patients. However, targeting PRMT5 stimulated ferritinophagy signaling and promoted the ferroptosis of HCC. PRMT5/ferritinophagy signaling may be a potential target for HCC.

Materials and methods

Specimen

Clinical samples were collected from HCC patients (n = 112) at Renmin Hospital of Wuhan University from July 2020, to June, 2022. Tissues were stored in liquid nitrogen at -80°C. This study was supported by the Ethical Committee of Renmin Hospital of Wuhan University (WDRY2023-K036). The informed consent was provided by the participants.

Immunohistochemistry assay

Tissues were cut into slides at the thickness of 4 μm. The slides were fixed in paraffin, deparaffinized and immersed in ethylene diamine tetraacetic acid buffer. After blocked with 1% bovine serum albumin (BSA) regents, the sections were incubated with primary antibodies. Afterwards, the sections were counterstained with 4',6-diamidino-2-phenylindole (DAPI). Subsequently, the sections were captured using a microscope (×200 magnification, Leica, Germany).

Cell culture

HEK293T cells, human HCC cell line Huh7, and liver epithelial cells (THLE-3) were provided by ATCC, USA. Cells were cultured in a Dulbecco's modified Eagle's medium containing 10% fetal bovine serum (FBS). Cells were incubated at 37°C in 5% CO_2.

Huh7 cells were exposed to 3 μM erastin (a ferroptosis inducer), 1 μM ferrostatin-1 (Fer-1, a ferroptosis inhibitor), 5 μM Z-VAD-FMK (a pan-caspase inhibitor), 5 mM GI-Y1 (an inhibitor of GSDMD) and necrosulfonamide (a necroptosis inhibitor).

Measurement of lipid peroxidation

Huh7 cells were incubated in serum-free DMEM using 3 μM C11-BODIPY 581/591 (Invitrogen, USA), washed three times with serum-free medium, trypsinized, resuspended in PBS, and detected by flow cytometry.

Determination of malondialdehyde (MDA), glutathione (GSH), and Fe^{2+} levels

The release of MDA and Fe^{2+} was determined using corresponding kits (Abcam, USA).

Reverse transcription-quantitative polymerase chain reaction (RT-qPCR)

Cells were lysed and RNAs were harvested. cDNA synthesis was conducted by a cDNA synthesis kit (18090010; Thermo Fisher Scientific, USA). PCR was conducted by an RT-PCR kit (12597500; Thermo Fisher Scientific, USA). Glyceraldehyde-3-phosphate dehydrogenase (GAPDH) was used as the loading control. mRNA was calculated using $2^{-\Delta\Delta Ct}$ methods.

Western blot

Total proteins were harvested from cells. Bicinchoninic acid assay was conducted to calculate protein concentration. 40 μg of protein was separated using 10% sodium dodecyl sulfate-polyacrylamide gel electrophoresis at 120 v and moved onto polyvinylidene fluoride (PVDF) membranes. After blocked with 5% non-fat milk, the membranes were incubated with primary antibodies, such as PRMT5 (ab109451; 1:10000, Abcam, UK), tumor protein p53 (TP53) (ab32049; 1:1000, Abcam, UK), H4R3me2s (ab309354; 1:1000, Abcam, UK), H3R8me2s (ab130740; 1:1000, Abcam, UK), GPX4 (ab125066; 1:1000, Abcam), RBM15 (ab315456; 1:1000, Abcam, UK), FTL (ab109373; 1:1000, Abcam, UK), FTH1 (ab183781; 1:1000, Abcam, UK), and β-actin (ab213262; 1:3000, Abcam, UK). Then the membranes were incubated with secondary antibodies (ab205718; 1:10000, Abcam, UK). Subsequently, the bands were imaged with an electrochemiluminescence kit (ab133406; Abcam, USA).

Cell Counting Kit-8 (CCK-8) assay

Cells were seeded into 96-well plates. Afterwards, cells were supplemented with CCK-8

solutions and cultured for 48 h. Finally, optic values were detected by Multiskan SkyHigh microplate reader (A51119500C; Thermo Fisher Scientific Inc., USA) at the wavelength of 450 nm.

Propidium iodide (PI) staining

After fixation in 4% paraformaldehyde and permeabilization with 0.2% Triton X-100, cells were blocked with 5% bovine serum. Then cells were stained with PI. The image was pictured by a microscope (×200 magnification, Leica, Germany).

N6-methyladenosine (m6A) dot blot assay

Total RNA was purified and spotted on onto cell membranes, which were then incubated with m6A antibody (ab284130; 1:5000, Abcam, UK) and anti-IgG (ab172730; 1:1000, Abcam, UK). Afterwards, the membranes were pictured using Tanon 5200 imaging system (Tanon, China).

Determination of m6A levels

m6A levels were calculated by an m6A RNA Methylation Kit (Colorimetric) (ab233491; Abcam, UK).

Methylated RNA immunoprecipitation (MeRIP) assay

MeRIP assay was performed using a Magna MeRIP™ m6A Kit (17-10499; Sigma-Aldrich, Germany). After transfection, cells were lysed. Then the cells were centrifugated and incubated with Protein-A/G agarose beads supplemented with antibodies against m6A (ab284130; 1:50, Abcam, UK) or IgG (ab172730; 1:50, Abcam, UK). Then the precipitate was collected, centrifuged, and mixed with elution buffer for 90 min at 50°C. The bound RNA was eluted ad purified. The purified RNA fragments were used for qPCR assay.

Luciferase assay

The fragments of PRMT5 were cloned into the pGL3-Basic vector (Promega Corporation). Subsequently, cells were co-transfected with wild/mutant type of PRMT5 or the control. The results were detected using a luciferase assay kit (E1501; Promega, USA).

Chromatin immunoprecipitation (ChIP) assay

ChIP assay was conducted using a Simple-ChIP® Enzymatic Chromatin IP Kit (CST, Boston, USA). Cells were sonicated to 400-800 bp. Then Chromatin was immunoprecipitated with protein-A/G-agarose gel beads conjugated with antibodies against TP53 (ab237976; 1:50, Abcam, UK) and IgG (ab172730; 1:50, Abcam, UK). The immunoprecipitated DNA was purified and analyzed by real-time PCR.

Glutathione-S-transferase (GST) pull-down assay

Recombinant proteins were prepared from BL21 E. coli. GST or GST-PRMT5 fusion proteins incubated with glutathione agarose (Roche, Switzerland). Afterwards, the GST fusion proteins were pictured using Coomassie brilliant blue. The binding proteins were subjected to western blot incubated with anti-His-tag mAb (Sigma-Aldrich, Germany).

Co-immunoprecipitation (Co-IP) assay

Nuclear extracts were extracted from cells. Then the nuclear extracts were incubated with antibodies against FLAG M2 agarose affinity gel, RNA binding motif protein 15 (RBM15) (ab70549; 1:100, Abcam, UK) or IgG (ab172730; 1:200, Abcam, UK). Afterwards, the mixtures were collected and washed with PBS. Subsequently, the immunocomplexes were subjected to western blot.

Xenograft assay

C57BL/6 nude mice (8-10 weeks, 18-23 g) were provided by Experimental Animal Center of Wuhan University. Mice were randomly divided into 4 groups: shNC group, shPRMT5 group, shPRMT5+Lv-NC group, shPRMT5+RBM15 group, dimethyl sulfoxide (DMSO) group, and GSK3326595 (GSK) group. Huh7 cells stably expressing PRMT5 shRNA and/or RBM15 were subcutaneously injected and planted into mice. For mice in DMSO and GSK group, mice were administrated with DMSO (1%, Solarbio, Beijing, China) or GSK (50 mg/kg) (EPZ015938; MCE, USA) [15]. At day 29, all mice were euthanized under isoflurane deep anesthesia. The tumor volume was determined every 7 days. The present study was approved by the Animal

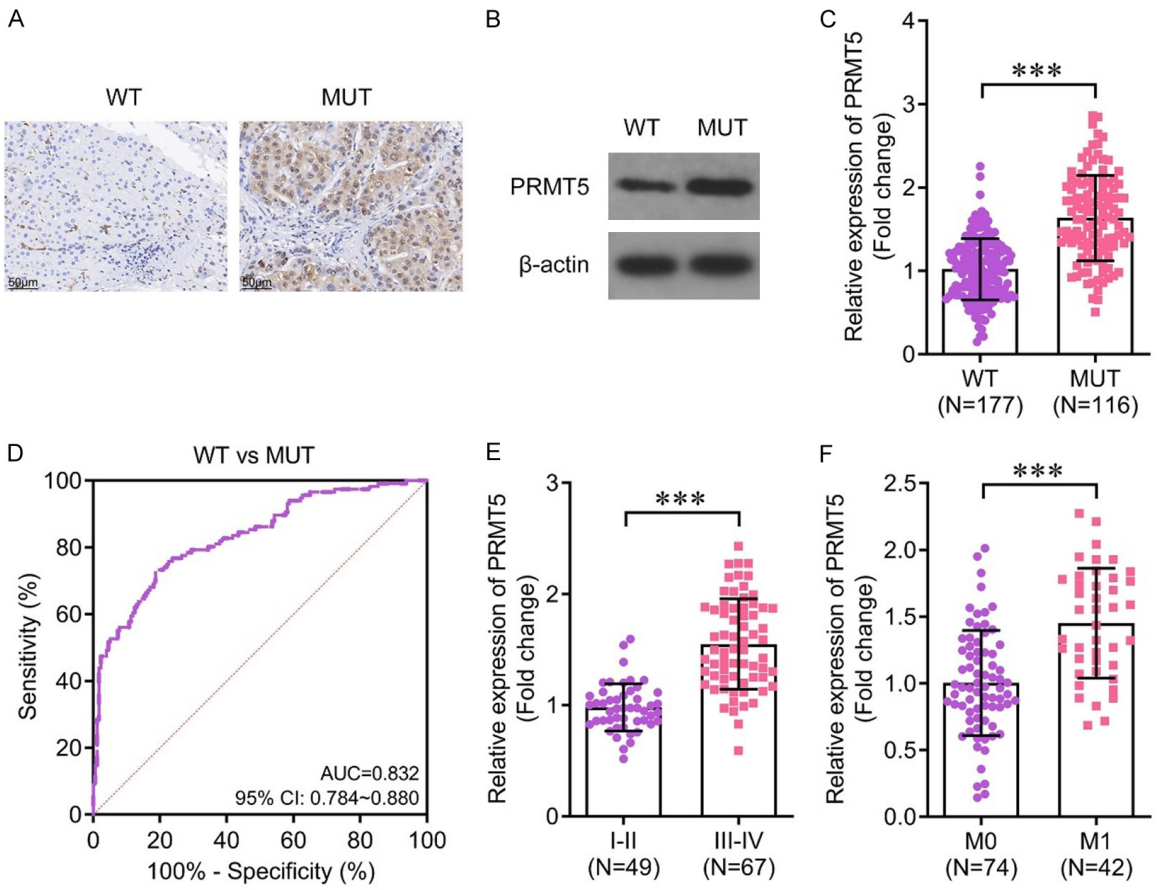

Figure 1. PRMT5 is upregulated in TP53-mutated HCC. A. PRMT5 expression was detected using immunohistochemistry. × 200 magnification. Scale bar: 20 μm. B. PRMT5 protein expression was detected using western blot. C. PRMT5 mRNA expression was detected using RT-qPCR. D. PRMT5 mRNA expression in HCC patients was analyzed using ROC curve. E, F. Subtype analysis of PRMT5 mRNA expression in HCC patients was performed using RT-qPCR. ***P<0.001.

Care Aboard of Renmin Hospital of Wuhan University.

Statistical analysis

Each independent experiment was performed in triplicate. Graphpad v.9.5.1. was applied for analyzing data. Data were presented as mean ± standard deviation (SD). The comparison between two groups was analyzed using Student t-test. The comparison among multiple groups was analyzed using ANOVA followed by Turkey's post hoc test. P<0.01 was deemed statistically important.

Results

PRMT5 is upregulated in TP53-mutated HCC

TP53 mutation induces genetic alteration during carcinogenesis [16]. PRMT5, a regulator of arginine methylation, is frequently abnormally expressed in cancer [17]. PRMT5 expression was obviously increased in TP53-mutated HCC tumor samples (**Figure 1A**). Both the protein and mRNA expression of PRMT5 was significantly increased in TP53-mutated HCC tumor samples (**Figure 1B**, **1C**). PRMT5 mRNA levels can be a prognostic marker of TP53-mutated HCC patients (**Figure 1D**). Overexpressed PRMT5 predicted advanced stages and distant metastasis (**Figure 1E**, **1F**).

TP53 epigenetically downregulates PRMT5

We found that TP53 was downregulated in TP53-mutated HCC tumor samples (**Figure 2A**). Moreover, in TP53-mutated HCC tumor samples, the protein expression of TP53 was obviously decreased (**Figure 2B**), whereas the global levels of H4R3me2s and H3R8me2s

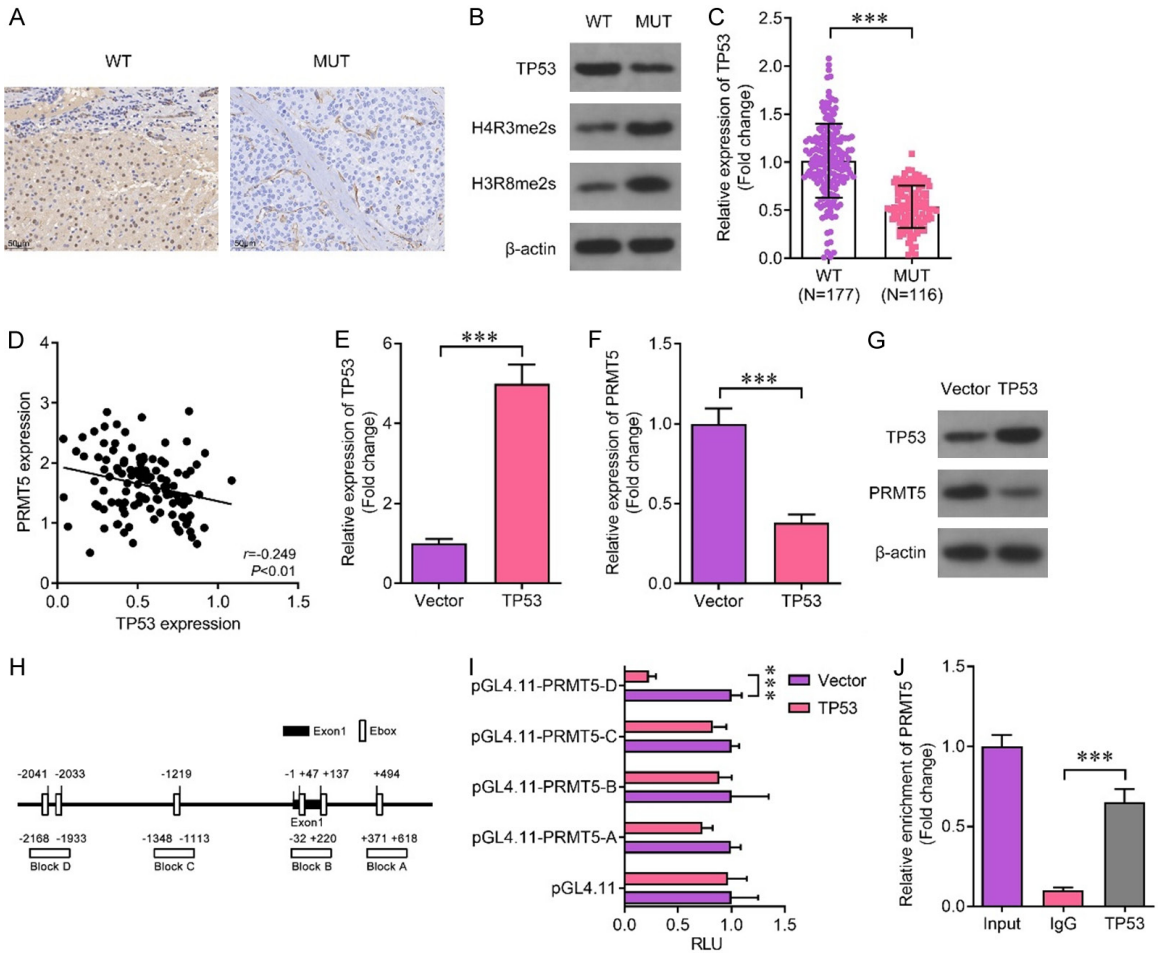

Figure 2. TP53 epigenetically downregulates PRMT5. A. TP53 expression was detected using immunohistochemistry. × 200 magnification. Scale bar: 50 μm. B. Protein expression was determined using western blot. C. TP53 mRNA expression in HCC patients was detected using RT-qPCR. D. Correlation between PRMT5 and TP53 was determined using Pearson analysis. E. TP53 mRNA expression in HCC cells was detected using RT-qPCR. F. PRMT5 mRNA expression in HCC cells was detected using RT-qPCR. G. Protein expression was determined using western blot. H, I. The interaction between PRMT5 and TP53 was confirmed by luciferase assay. J. The enrichment of TP53 in the promoter of PRMT5 was detected using ChIP assay. ***P<0.001, ***P<0.001.

was decreased. Then we analyzed mRNA expression of TP53 and PRMT5 in HCC patients. TP53 was obviously downregulated in TP53-mutated HCC tumor samples (**Figure 2C**). Moreover, PRMT5 and TP53 expression was in negative correlation (**Figure 2D**). TP53 was overexpressed by its overexpression plasmids (**Figure 2E**), suggesting that cells were successfully transfected. Overexpression of TP53 significantly inhibited the mRNA expression of PRMT5 (**Figure 2F**). This is paralleled with western blot (**Figure 2G**). As a transcription factor, TP53 regulates gene expression via targeting the promoter of downstream. We found that there were four putative E-boxes in the promoter of PRMT5 (**Figure 2H**). The E-box inserted into the luciferase reporter. Then cells were transfected with the pGL4.11 reporter and TP53 overexpression plasmids or its vector. We found that overexpression of TP53 significantly increased the luciferase activity at Block C, but not A, B, and D (**Figure 2I**), suggesting that TP53 may regulate PRMT5 expression via binding to C. Moreover, overexpression of TP53 significantly promoted its enrichment in the promoter of PRMT5 (**Figure 2J**).

PRMT5 knockdown promotes the ferroptosis of HCC

Targeting PRMT5 inhibits the progression of multi-type cancers [18]. To confirm the roles of

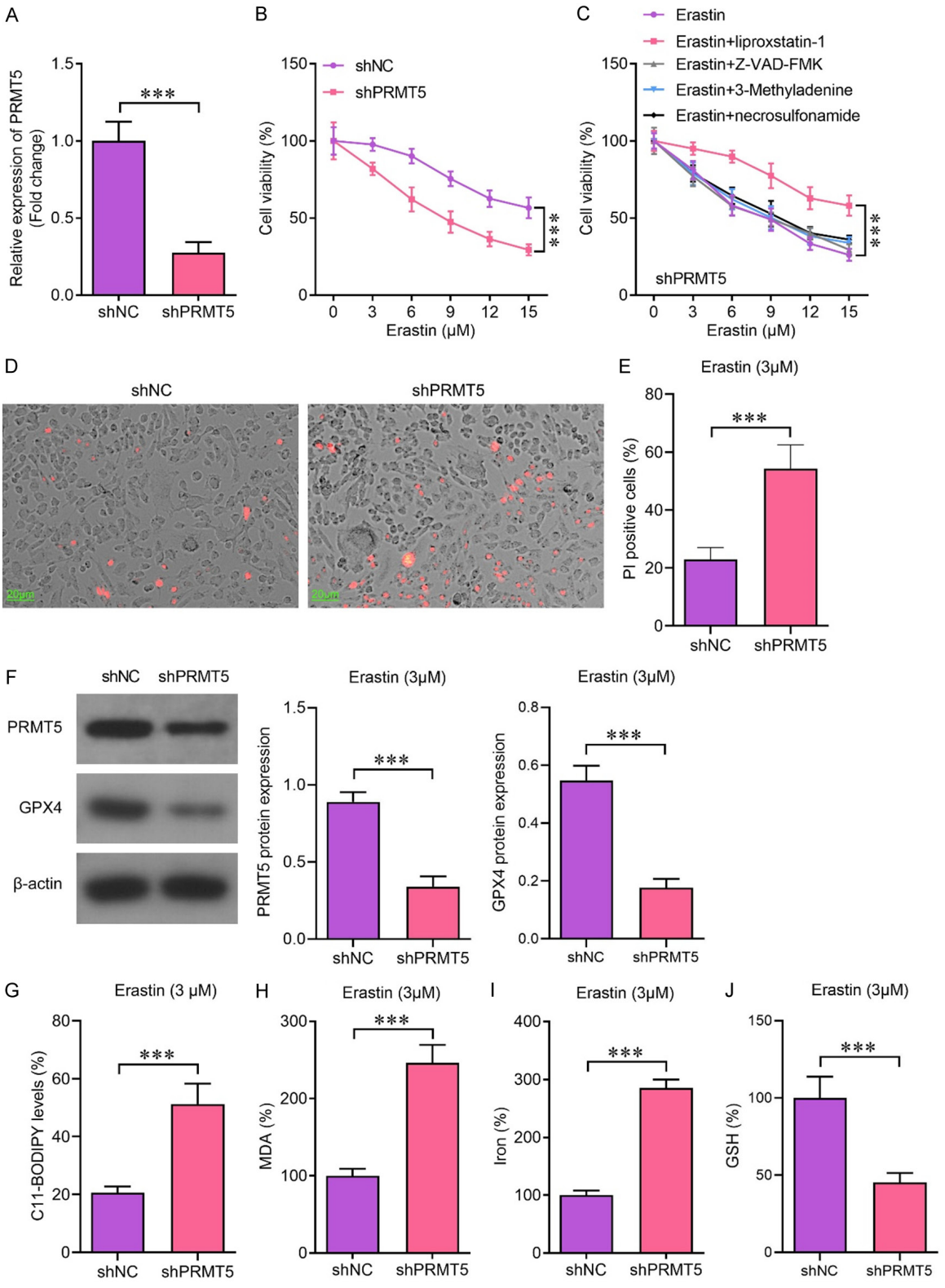

Figure 3. PRMT5 knockdown promotes the ferroptosis of HCC. (A) PRMT5 mRNA expression in HCC cells was detected using RT-qPCR. (B, C) Cell viability was determined using CCK-8 assay. (D, E) Cell death was detected using PI staining. × 200 magnification. Scale bar: 20 μm. (F) Protein expression was determined using western blot. The levels of C11-BODIPY (G), MDA (H), iron (I) and GSH (J). ***P<0.001.

PRMT5 in HCC, cells were transfected with PRMT5 shRNAs. **Figure 3A** showed that PRMT5 shRNAs, especially sh2, significantly decreased PRMT5 mRNA expression. PRMT5 knockdown significantly inhibited the cell viability of HCC cells compared with shNC group (**Figure 3B**). To confirm which form of death involved in PRMT5 shRNA-mediated death of HCC, cells were exposed to erastin, Fer-1, Z-VAD-FMK, 5 mM 3-Methyladenine on the background of shPRMT5 transfection. The results showed that Lip-1 significantly alleviated the effects of erastin and promoted the cell viability of HCC cells, whereas Z-VAD-FMK, 3-MA, and NSC showed no obvious effects (**Figure 3C**). PRMT5 knockdown significantly increased the percentages of PI positive cells (**Figure 3D**, **3E**) Moreover, PRMT5 knockdown significantly inhibited the expression of PRMT5 and glutathione peroxidase 4 (GPX4) (**Figure 3F**). PRMT5 knockdown also increased the levels of C11-BODIPY, MDA and ferrous iron (Fe^{2+}) (**Figure 3G-I**), whereas decreasing GSH levels (**Figure 3J**).

PRMT5 interacts with RBM15

m6A modification is involved in the processes of ferroptosis [19-21]. Thence we hypothesized that PRMT5 may inhibit ferroptosis of HCC cells via binding to RNA methylation regulator. We found that His-tagged PRMT5 could interact with GST-tagged RBM15 (**Figure 4A**, **4B**). PRMT5 could bind to bound to RBM15 (**Figure 4C**, **4D**). FLAG-tagged PRMT5 is associated HA-tagged RBM15 in HEK293T cells (**Figure 4E**, **4F**). Co-IP further confirmed the interaction between PRMT5 and RBM15 (**Figure 4G**). Moreover, ferroptosis inhibitor Fer-1 promoted the enrichment of PRMT5 in the promoter of NRF2 (oxidative stress), GPX4 (lipid peroxidation), and FTH1 (iron metabolism), especially FTH1 (**Figure 4H**), which was reversed by RBM15 knockdown. H3R2 dimethylation at the promoter of NFE2 like bZIP transcription factor 2 (NRF2), GPX4, and FTH1 was also reversed by RBM15 knockdown (**Figure 4I**). As the alteration of FTH1 was more remarkable. Therefore, FTH1 was chosen for further study.

PRMT5/RBM15 axis regulates m6A modification of FTH1

RBM15, a m6A "writer", is involved in m6A modification of its target [22]. Therefore, we further investigated the m6A modification of FTH1 by RBM15. RBM15 expression was obviously increased in HCC cells (**Figure 5A**). Overexpressed RBM15 significantly increased the protein expression of FTH1 and FTH1 (**Figure 5B**). Moreover, overexpressed RBM15 significantly increased the m6A levels of FTH1 (**Figure 5C**, **5D**). The online database SRAMP showed that there were 4 m6A sites with high confidence in human liver (**Figure 5E**). **Figure 5F** showed the second structure of 4 m6A sites. The m6A enrichment of FTH1 was increased at sites Site1, 2, and 4 (**Figure 5G**), whereas showing no significant alteration at Site3. Moreover, overexpressed RBM15 significantly increased the m6A enrichment at site Site4 (**Figure 5H**), but not site Site1, 2, and 3. Therefore, we hypothesized that RBM15 may regulate m6A modification of FTH1 via binding to site4. To confirm this, we mutated Site4 from GAACU into CUUGA. **Figure 5I** showed the transfection efficiency of RBM15 shRNA and overexpression plasmids. We found that overexpressed RBM15 significantly increased the luciferase activity (**Figure 5J**), while RBM15 exerted the opposite effects. We also found that PRMT5 knockdown mediated inhibition in the mRNA expression and stability of FTH1 was significantly reversed by overexpressed RBM15 (**Figure 5K**, **5L**). These findings suggested that PRMT5 interacted with RBM15 to regulate FTH1 expression.

FTH1 overexpression inhibits the ferroptosis of HCC

To confirm the roles of PRMT5/FTH1 axis in HCC, cells were transfected with (**Figure 6A**). Overexpressed RBM15 significantly antagonized the effects of PRMT5 knockdown and promoted the cell survival of HCC cells (**Figure 6B**). Overexpressed FTH1 also inhibited the death of HCC cells (**Figure 6C**, **6D**). Moreover, overexpression obviously inhibited the protein expression of FTL and FTH1 (**Figure 6E**). Moreover, overexpressed FTH1 significantly reduced the levels of C11-BODIPY, MDA, and Fe^{2+} levels (**Figure 6F-H**), while increasing GSH levels (**Figure 6I**).

PRMT5/FTH1 axis promotes tumor growth and inhibits ferroptosis in vivo

In vivo assays were performed to further verify the roles of PRMT5/FTH1 axis in HCC. We found that PRMT5 knockdown significantly inhibited the tumor growth of HCC, which was antago-

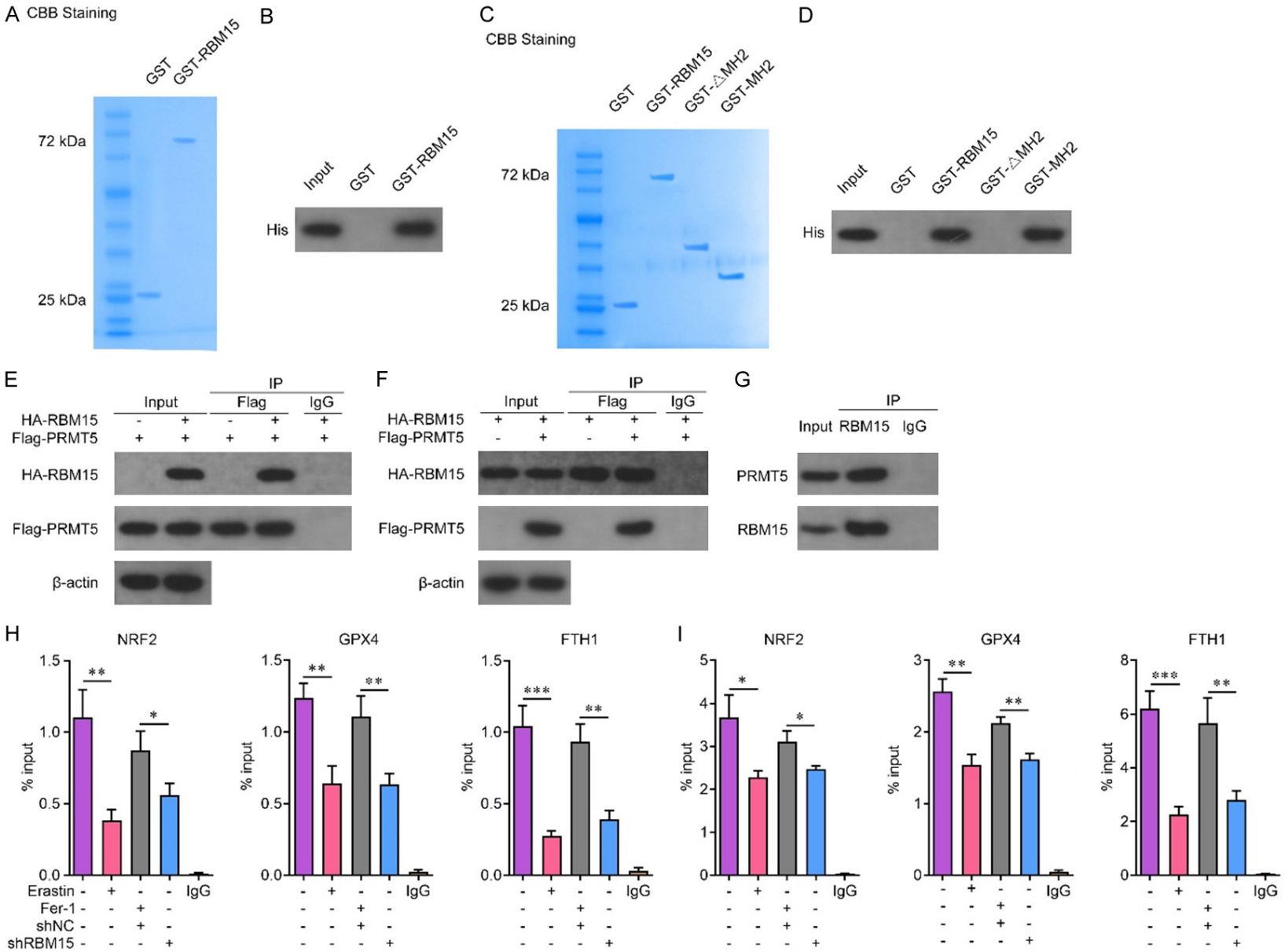

Figure 4. PRMT5 interacts with RBM15. (A-D) The interaction between PRMT5 and RBM15 was determined using CST pull-down assay. (E-G) The interaction between PRMT5 and RBM15 was confirmed using Co-IP assay. The enrichment of PRMT5 (H) and H3R2me2 (I) in the enrichment of RBM15 was determined using ChIP assay. **P*<0.05, ***P*<0.01, ****P*<0.001.

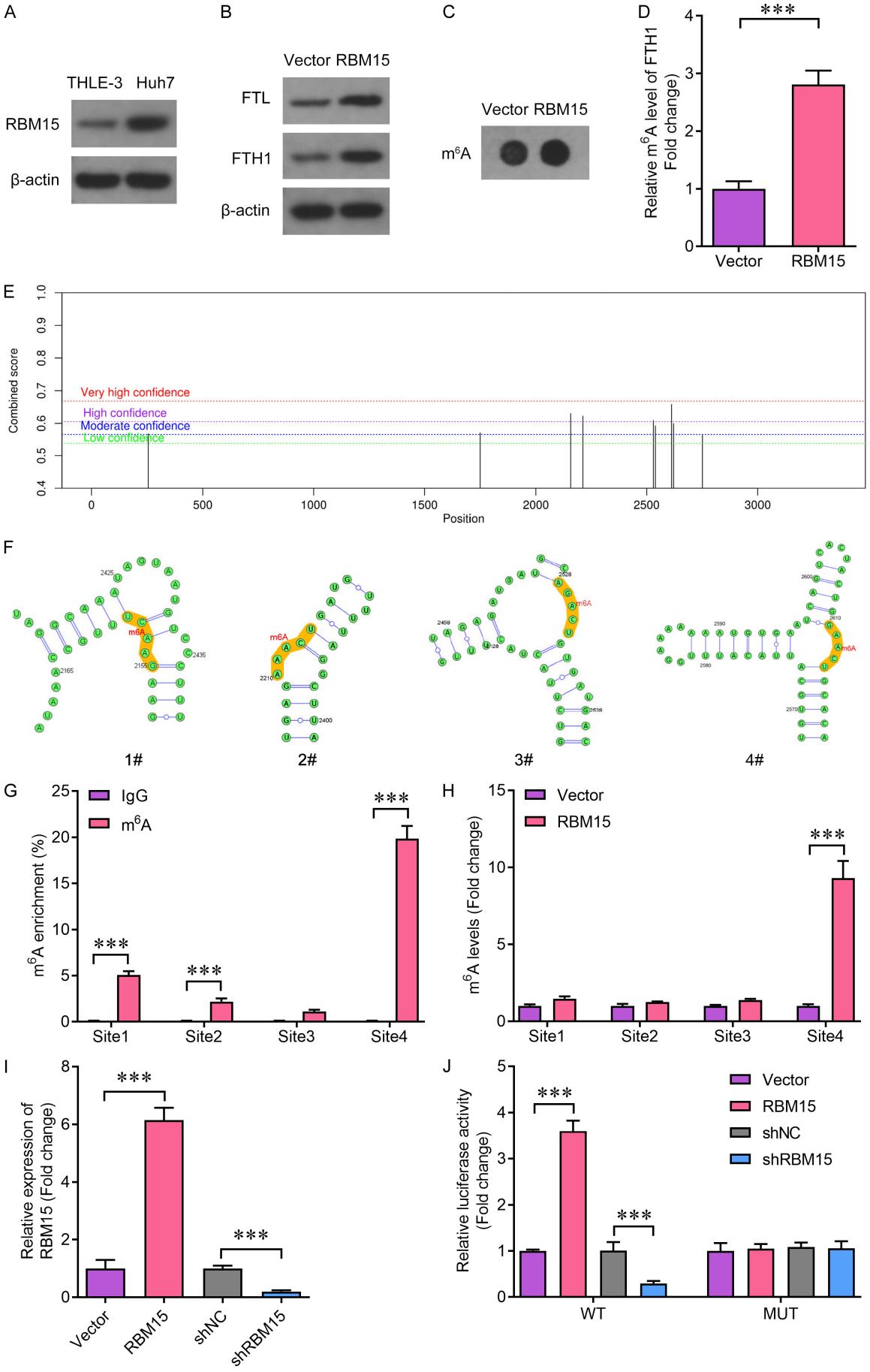
A
THLE-3 Huh7
RBM15
β-actin
B
Vector RBM15
FTL
FTH1
β-actin
C
Vector RBM15
m6A
D
***
Relative m6A level of FTH1 Fold change)
Vector
RBM15
E
Combined score
Very high confidence
High confidence
Moderate confidence
Low confidence
Position
F
1#
2#
3#
4#
G
IgG
m6A
m6A enrichment (%)
***
Site1
Site2
Site3
Site4
H
Vector
RBM15
m6A levels (Fold change)
***
Site1
Site2
Site3
Site4
I
Relative expression of RBM15 (Fold change)
***
***
Vector
RBM15
shNC
shRBM15
J
Vector
RBM15
shNC
shRBM15
Relative luciferase activity (Fold change)
***
***
WT
MUT

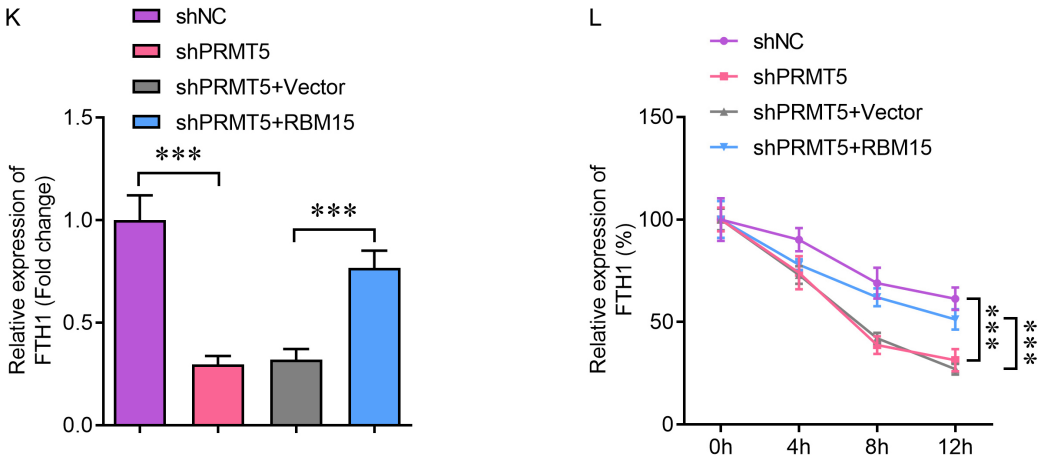

Figure 5. PRMT5/RBM15 axis regulates m6A modification of FTH1. A. RBM15 protein expression was determined using western blot. B. Protein expression was determined using western blot. C. Total m6A levels were determined using m6A dot blot assay. D. The m6A levels of FTH1 was detected using m6a assay. E. The m6A sites of FTH1 were predicted using the online database SRAMP. F. The second structure of the m6Awas analyzed using SRAMP. G. m6A enrichment of FTH1 was determined using MeRIP assay. H. The m6A levels of FTH1 was detected using m6a assay. I. RBM15 mRNA expression was determined using RT-qPCR. J. The interaction between RBM15 and FTH1 was confirmed using luciferase assay. K. FTH1 mRNA expression was determined using RT-qPCR. L. FTH1 mRNA stability was determined using RT-qPCR. ***P<0.001.

nized by overexpressed FTH1 (**Figure 7A-C**). Overexpressed FTH1 increased the expression of Ki-67 compared with shPRMT5 + vector group (**Figure 7D**), whereas downregulating 4-HNE. Overexpressed FTH1 significantly increased the levels of C11-BODIPY compared with shPRMT5 + vector group (**Figure 7E**, **7F**), suggesting that FTH1 inhibits lipid peroxidation *in vivo*. Additionally, overexpressed FTH1 significantly suppressed the release of MDA and iron compared with shPRMT5 + vector group (**Figure 7G**, **7H**), while increasing GSH levels (**Figure 7I**). These results suggested that PRMT5/FTH1 axis promotes the tumor growth and suppresses ferroptosis of HCC.

GSK inhibits tumor growth and promotes ferroptosis in HCC

To further confirm the role of PRMT5 in HCC, mice were administrated with PRMT5 inhibitor GSK3326595 (GSK). We found that GSK treatment significantly reduced the tumor size, weight, and volume (**Figure 8A-C**). GSK treatment markedly reduced the expression of Ki-67, whereas upregulating 4-HNE (**Figure 8D**). GSK treatment significantly promoted lipid peroxidation (**Figure 8E**, **8F**). Moreover, GSK treatment significantly promoted accumulation of MDA and iron (**Figure 8G**, **8H**), whereas reducing the levels of GSH (**Figure 8I**). These results suggested that inhibition of PRMT5 suppresses tumor growth and promotes ferroptosis of HCC.

Discussion

The alteration of PTMs is a hallmark of carcinogenesis [23-25]. As a common pattern of PTMs, arginine methylation is involved in the initiation and progression of multi-type cancers, including HCC [11, 26-28]. In this study, high levels of PRMT5 predicted poor clinical outcomes of HCC patients. PRMT5 interacted with RBM15 to promote m6A modification of FTH1, which induced the upregulation of FTH1. Interestingly, PRMT5 knockdown promoted ferritinophagy and ferroptosis of HCC cells.

PRMT5 functions as an oncogene in multitype cancers. For instance, PRMT5 promotes TCA cycle and tumor growth of ovarian cancer [29]. PRMT5 mediates m6A demethylation and neutralizes the efficacy of doxorubicin in breast cancer [30]. Kim et al. [31] also demonstrate that PRMT5 reprograms tumor microenvironment, resulting in immunosuppression. In the progression of HCC, overexpression of PRMT5 promotes the aggressiveness of HCC cells, enhances sorafenib resistance, and induces immune silence [14, 15, 32], indicating that its oncogenic role in HCC. Therefore, PRMT5 has

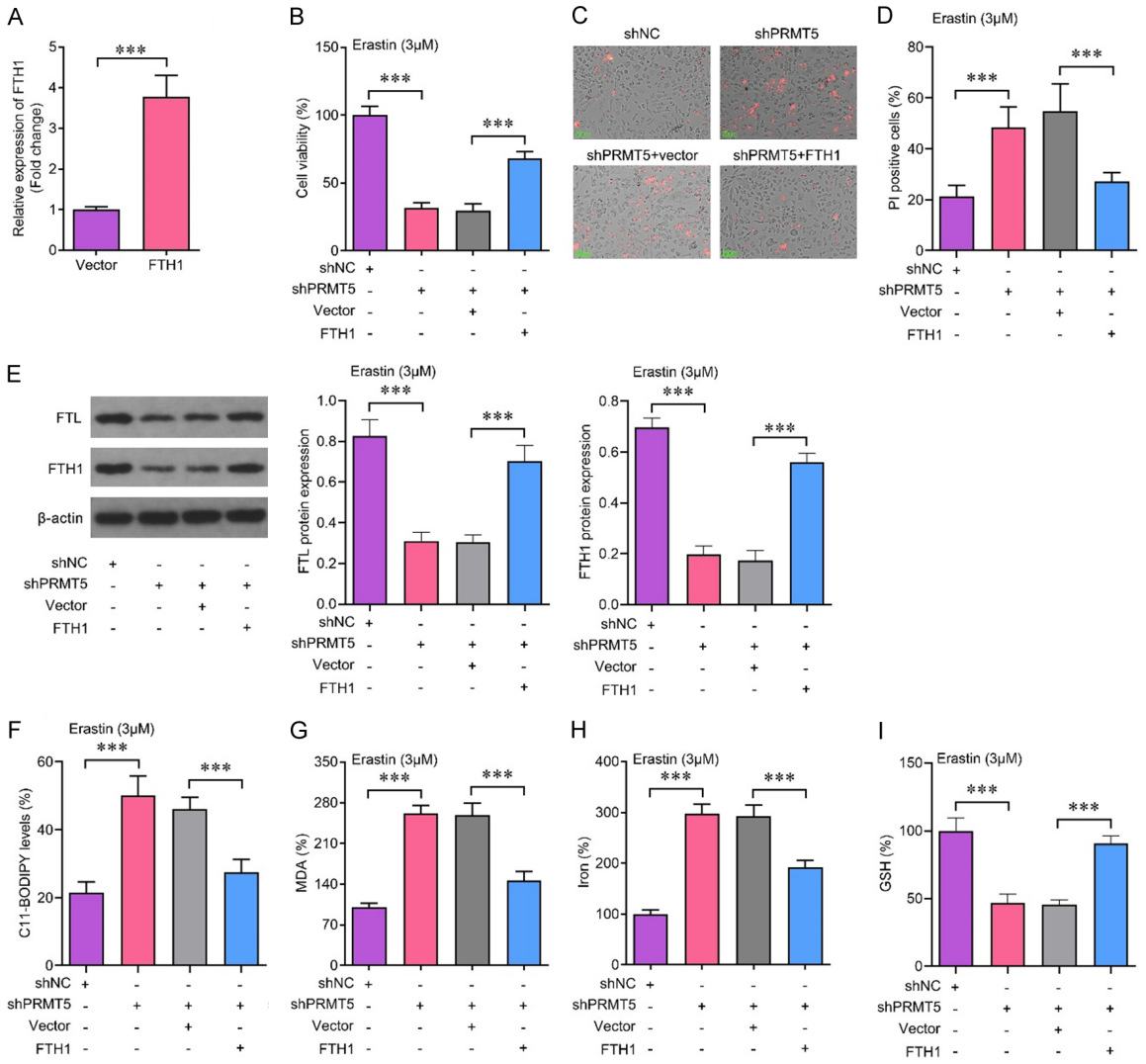

Figure 6. FTH1 overexpression inhibits the ferroptosis of HCC. (A) FTH1 mRNA expression in HCC cells was detected using RT-qPCR. (B, C) Cell viability was determined using CCK-8 assay. (C, D) Cell death was detected using PI staining. × 200 magnification. Scale bar: 20 μm. (E) Protein expression was determined using western blot. The levels of C11-BODIPY (F), MDA (G), iron (H) and GSH (I). ***P<0.001.

been demonstrated as a potential target for HCC. Engstrom et al. evidence that clinical-use of 5'-deoxy-5'-methylthioadenosine-cooperative PRMT5 inhibitor MRTX1719 suppresses the progression of methylthioadenosine phosphorylase-deleted tumors [33]. In this study, PRMT5 predicted poor clinical outcomes of HCC patients. Interestingly, targeting PRMT5 by its specific shRNA or inhibitor promoted ferroptotic death of HCC cells and suppressed tumor growth. These findings suggested that targeting PRMT5 may be a promising strategy for HCC.

m6A methylation is the most common RNA modification in eukaryotic cells. However, aberrant m6A methylation promotes the proliferation, differentiation, metabolic imbalance, immunosuppression of tumor [34]. m6A modification is regulated by m6A methyltransferases (methyltransferase 3/14/16, RBM15/15B, etc.), m6A demethyltransferases (FTO alpha-ketoglutarate dependent dioxygenase and alkB homolog 5), as well as m6A RNA binding proteins (insulin like growth factor 2 mRNA binding protein 1/2/3, YTH N6-methyladenosine RNA binding protein F1/2/3, etc.) [35]. RBM15 has been identified as a prognostic biomarker of HCC patients [36]. Cai et al. [37] also report that overexpressed RBM15 contributes to the invasiveness of HCC cells. In this study, PRMT5 interacted with RBM15 to induce its upregula-

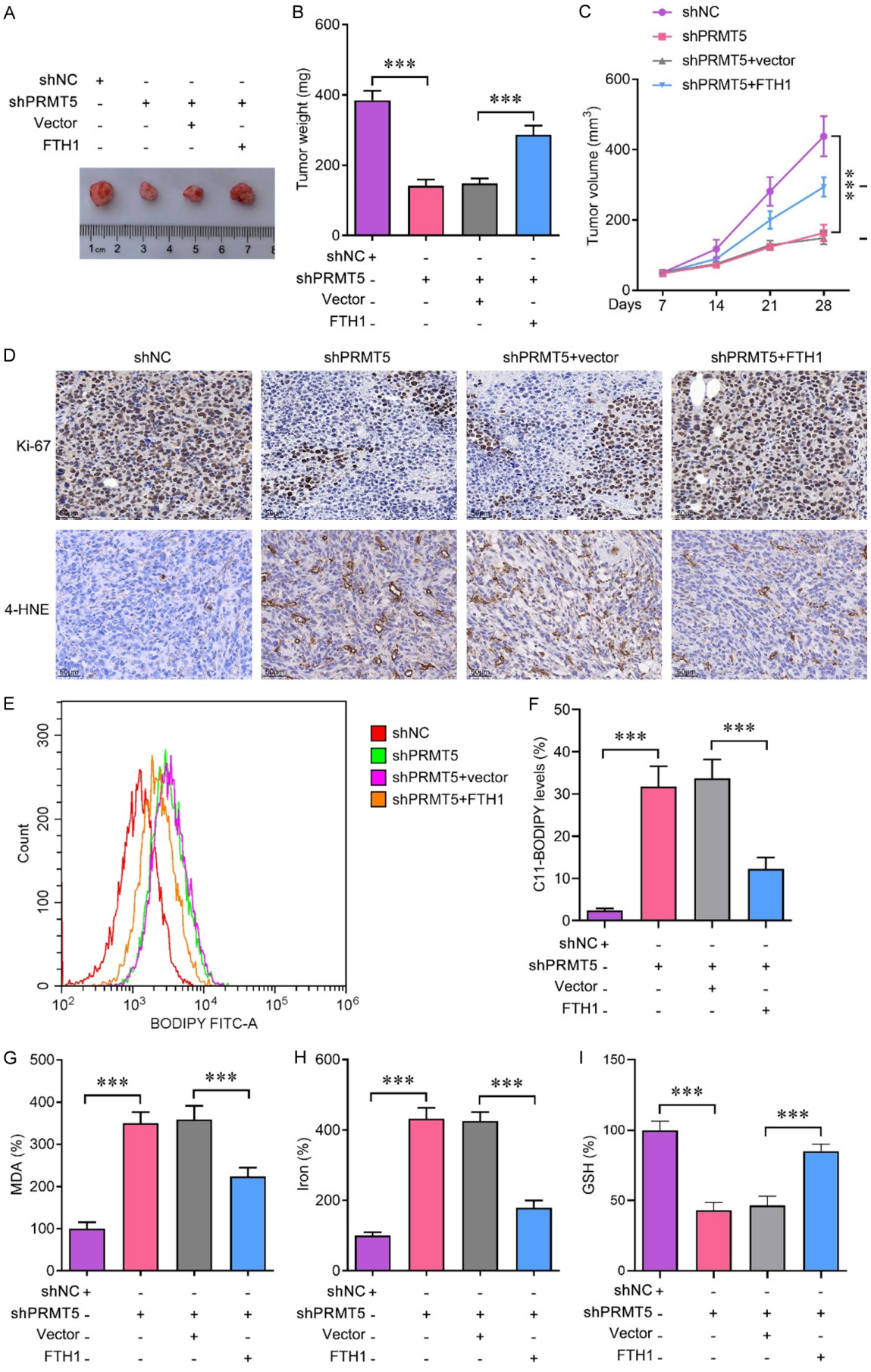
A
shNC + - - -
shPRMT5 - + + +
Vector - - + -
FTH1 - - - +
B
Tumor weight (mg)
600
400
200
0
***
***
shNC + - - -
shPRMT5 - + + +
Vector - - + -
FTH1 - - - +
C
shNC
shPRMT5
shPRMT5+vector
shPRMT5+FTH1
Tumor volume (mm3)
600
400
200
0
Days 7 14 21 28
***
D
shNC
shPRMT5
shPRMT5+vector
shPRMT5+FTH1
Ki-67
4-HNE
E
Count
300
200
100
0
10^2 10^3 10^4 10^5 10^6
BODIPY FITC-A
shNC
shPRMT5
shPRMT5+vector
shPRMT5+FTH1
F
C11-BODIPY levels (%)
50
40
30
20
10
0
***
***
shNC + - - -
shPRMT5 - + + +
Vector - - + -
FTH1 - - - +
G
MDA (%)
500
400
300
200
100
0
***
***
shNC + - - -
shPRMT5 - + + +
Vector - - + -
FTH1 - - - +
H
Iron (%)
600
400
200
0
***
***
shNC + - - -
shPRMT5 - + + +
Vector - - + -
FTH1 - - - +
I
GSH (%)
150
100
50
0
***
***
shNC + - - -
shPRMT5 - + + +
Vector - - + -
FTH1 - - - +

Figure 7. PRMT5/FTH1 axis promotes tumor growth in vivo. The tumor size (A), weight (B), and volume (C) was determined using xenograft assay. (D) Ki-67 expression was detected using immunohistochemistry. ×200 magnification. Scale bar: 50 μm. The release of C11-BODIPY (E, F), MDA (G), iron (H), and GSH (I). ***P<0.001.

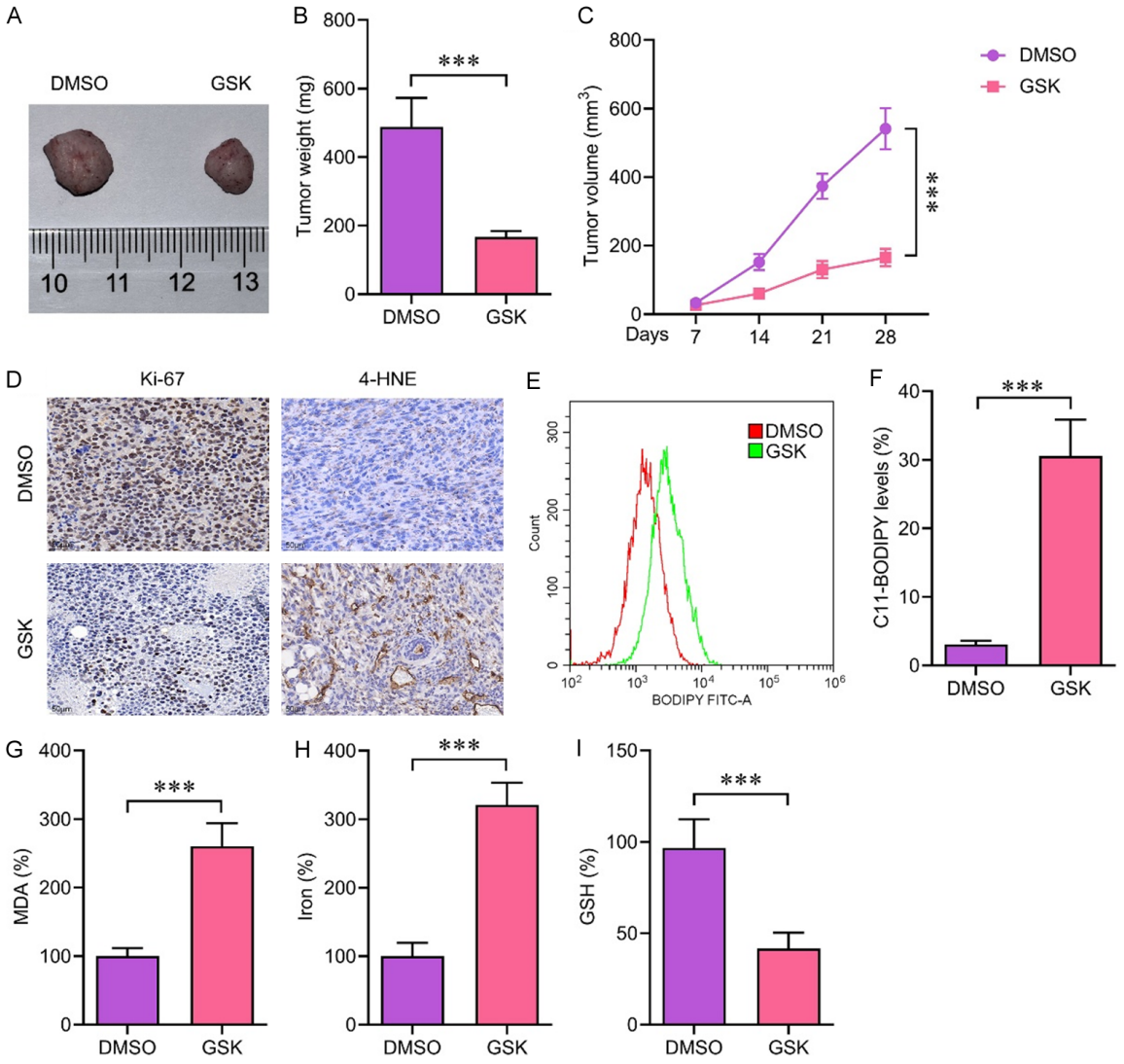

Figure 8. GSK inhibits tumor growth and mediates ferroptosis of HCC in vivo. The tumor size (A), weight (B), and volume (C) was determined using xenograft assay. (D) Ki-67 expression was detected using immunohistochemistry. ×200 magnification. Scale bar: 50 μm. The release of C11-BODIPY (E, F), MDA (G), iron (H), and GSH (I). ***P<0.001.

tion. However, overexpression of RBM15 alleviated the effects of PRMT5 knockdown and suppressed the ferroptosis of HCC cells.

PRMT5 plays a key role in maintaining genome integrity [38]. However, its role in ferroptotic death is scarcely reported. In the present study, RBM15 acted as a novel PRMT5 substrate with arginine methylation. RBM15 functions as an oncogene in breast cancer, lung cancer, gastric cancer, as well as HCC [39-42]. RBM15-mediated m6A modification of its downstream contributes the aggressiveness of tumor cells [43]. We found that PRMT5 could interacted with RBM15 to mediate mRNA expression and stability of FTH1, which inhibits ferritinophagy and ferroptosis.

Ferroptosis is regulated by following three mechanisms: oxidative stress (NRF2), lipid per-

oxidation (solute carrier family 7 member 11, glutamate-cysteine ligase catalytic subunit, etc.), and iron metabolism (metallothionein 1G, FTH1, etc.) [6]. Increasing evidences have demonstrated that targeting the mechanisms by ferroptosis inducer suppresses the tumor growth [44, 45]. In this study, PRMT5 interacted with RBM15 to upregulate FTH1 expression, which inhibited the transport of iron and decreased the release of ferrous iron. This indicated the blockage of ferritinophagy, resulting in the inhibition of ferroptosis. Although oxidative stress and lysosomal toxicity may also induce other form of cell death, such as apoptosis, necroptosis, and ferroptosis [46-49]. However, ferroptosis is different from apoptosis and necroptosis in that apoptosis is characterized by caspase cascades and that necroptosis is featured by the assembly of necrosome, whereas ferroptosis is induced by iron-dependent lipid peroxidation [50]. In this study, the increase in MDA and ferrous iron indicated that the death of HCC cells was in ferroptotic form [51]. No alteration in cell viability after exposure to pan caspase inhibitor, 3-MA, and NCS further confirm this finding.

However, there are several limitations in this study. Firstly, the number of participants involved in this study is small. A larger population will make the results more convincing. As ferroptosis is regulated by the three mechanisms aforementioned, a single ferroptoitic inhibitor cannot be a convincing strategy to induce ferroptosis. In the scenario that oxidized PUFA-PLs decompose into reactive electrophiles that then damage other macromolecules, reactive electrophiles go for ferroptosis, while caspases mediate apoptosis [6]. That is to say, ferroptosis may be accompanied by cell apoptosis. How to identify the form of death in this condition? This needs further study.

Conclusion

In conclusion, PRMT5 functions as an oncogene in HCC. PRMT5 interacts with RBM15 to upregulate FTH1, inhibiting ferritinophagy and ferroptosis of HCC. Therefore, targeting PRMT5/RBM15/ferritinophagy signaling may be a potential target for HCC.

Acknowledgements

This work was supported by the National Natural Science Foundation of China (No. 31971166), Renmin Hospital of Wuhan University Interdisciplinary Innovation Talent Project Fund (No. JCRCYR-2022-015), and Hubei Provincial Natural Science Foundation (2025AFD794).

Disclosure of conflict of interest

None.

Address correspondence to: Ximing Xu, Cancer Center, Renmin Hospital of Wuhan University, No. 99 Zhangzhidong Road, Wuhan 430060, Hubei, China. Tel: +86-13707120651. E-mail: doctorxu120@aliyun.com

References

[1] Toh MR, Wong EYT, Wong SH, Ng AWT, Loo LH, Chow PK and Ngeow J. Global epidemiology and genetics of hepatocellular carcinoma. Gastroenterology 2023; 164: 766-782.

[2] Ladd AD, Duarte S, Sahin I and Zarrinpar A. Mechanisms of drug resistance in HCC. Hepatology 2024; 79: 926-940.

[3] Foerster F, Gairing SJ, Muller L and Galle PR. NAFLD-driven HCC: Safety and efficacy of current and emerging treatment options. J Hepatol 2022; 76: 446-457.

[4] Liang JY, Wang DS, Lin HC, Chen XX, Yang H, Zheng Y and Li YH. A novel ferroptosis-related gene signature for overall survival prediction in patients with hepatocellular carcinoma. Int J Biol Sci 2020; 16: 2430-2441.

[5] Duan H, Liu Y, Gao Z and Huang W. Recent advances in drug delivery systems for targeting cancer stem cells. Acta Pharm Sin B 2021; 11: 55-70.

[6] Jiang X, Stockwell BR and Conrad M. Ferroptosis: mechanisms, biology and role in disease. Nat Rev Mol Cell Biol 2021; 22: 266-282.

[7] Tang D, Chen X, Kang R and Kroemer G. Ferroptosis: molecular mechanisms and health implications. Cell Res 2021; 31: 107-125.

[8] Qin Y, Qiao Y, Wang D, Tang C and Yan G. Ferritinophagy and ferroptosis in cardiovascular disease: mechanisms and potential applications. Biomed Pharmacother 2021; 141: 111872.

[9] Wu J, Liu Q, Zhang X, Tan M, Li X, Liu P, Wu L, Jiao F, Lin Z, Wu X, Wang X, Zhao Y and Ren J. The interaction between STING and NCOA4 exacerbates lethal sepsis by orchestrating ferroptosis and inflammatory responses in macrophages. Cell Death Dis 2022; 13: 653.

[10] Zhang Z, Yao Z, Wang L, Ding H, Shao J, Chen A, Zhang F and Zheng S. Activation of ferritinophagy is required for the RNA-binding protein ELAVL1/HuR to regulate ferroptosis in hepatic

stellate cells. Autophagy 2018; 14: 2083-2103.
[11] Wu Q, Schapira M, Arrowsmith CH and Barsyte-Lovejoy D. Protein arginine methylation: from enigmatic functions to therapeutic targeting. Nat Rev Drug Discov 2021; 20: 509-530.
[12] Wang Y and Bedford MT. Effectors and effects of arginine methylation. Biochem Soc Trans 2023; 51: 725-734.
[13] Xu J and Richard S. Cellular pathways influenced by protein arginine methylation: implications for cancer. Mol Cell 2021; 81: 4357-4368.
[14] Zhou Z, Chen Z, Zhou Q, Meng S, Shi J, Mui S, Jiang H, Lin J, He G, Li W, Zhang J, Wang J, He C, Yan Y and Xiao Z. SMYD4 monomethylates PRMT5 and forms a positive feedback loop to promote hepatocellular carcinoma progression. Cancer Sci 2024; 115: 1587-1601.
[15] Luo Y, Gao Y, Liu W, Yang Y, Jiang J, Wang Y, Tang W, Yang S, Sun L, Cai J, Guo X, Takahashi S, Krausz KW, Qu A, Chen L, Xie C and Gonzalez FJ. Myelocytomatosis-protein arginine n-methyltransferase 5 axis defines the tumorigenesis and immune response in hepatocellular carcinoma. Hepatology 2021; 74: 1932-1951.
[16] Daver NG, Maiti A, Kadia TM, Vyas P, Majeti R, Wei AH, Garcia-Manero G, Craddock C, Sallman DA and Kantarjian HM. TP53-mutated myelodysplastic syndrome and acute myeloid leukemia: biology, current therapy, and future directions. Cancer Discov 2022; 12: 2516-2529.
[17] Zheng J, Li B, Wu Y, Wu X and Wang Y. Targeting arginine methyltransferase PRMT5 for cancer therapy: updated progress and novel strategies. J Med Chem 2023; 66: 8407-8427.
[18] Gao J, Yang J, Xue S, Ding H, Lin H and Luo C. A patent review of PRMT5 inhibitors to treat cancer (2018 - present). Expert Opin Ther Pat 2023; 33: 265-292.
[19] Zhang H, Wu D, Wang Y, Guo K, Spencer CB, Ortoga L, Qu M, Shi Y, Shao Y, Wang Z, Cata JP and Miao C. METTL3-mediated N6-methyladenosine exacerbates ferroptosis via m6A-IGF2BP2-dependent mitochondrial metabolic reprogramming in sepsis-induced acute lung injury. Clin Transl Med 2023; 13: e1389.
[20] Yang P, Yang W, Wei Z, Li Y, Yang Y and Wang J. Novel targets for gastric cancer: The tumor microenvironment (TME), N6-methyladenosine (m6A), pyroptosis, autophagy, ferroptosis and cuproptosis. Biomed Pharmacother 2023; 163: 114883.
[21] Zhang G, Mi W, Wang C, Li J, Zhang Y, Liu N, Jiang M, Jia G, Wang F, Yang G, Zhang L, Wang J, Fu Y and Zhang Y. Targeting AKT induced Ferroptosis through FTO/YTHDF2-dependent GPX4 m6A methylation up-regulating and degradating in colorectal cancer. Cell Death Discov 2023; 9: 457.
[22] Jiang X, Liu B, Nie Z, Duan L, Xiong Q, Jin Z, Yang C and Chen Y. The role of m6A modification in the biological functions and diseases. Signal Transduct Target Ther 2021; 6: 74.
[23] Chen L, Liu S and Tao Y. Regulating tumor suppressor genes: post-translational modifications. Signal Transduct Target Ther 2020; 5: 90.
[24] Chen N, Zheng Q, Wan G, Guo F, Zeng X and Shi P. Impact of posttranslational modifications in pancreatic carcinogenesis and treatments. Cancer Metastasis Rev 2021; 40: 739-759.
[25] Pan S and Chen R. Pathological implication of protein post-translational modifications in cancer. Mol Aspects Med 2022; 86: 101097.
[26] Dong H, He X, Zhang L, Chen W, Lin YC, Liu SB, Wang H, Nguyen LXT, Li M, Zhu Y, Zhao D, Ghoda L, Serody J, Vincent B, Luznik L, Gojo I, Zeidner J, Su R, Chen J, Sharma R, Pirrotte P, Wu X, Hu W, Han W, Shen B, Kuo YH, Jin J, Salhotra A, Wang J, Marcucci G, Luo YL and Li L. Targeting PRMT9-mediated arginine methylation suppresses cancer stem cell maintenance and elicits cGAS-mediated anticancer immunity. Nat Cancer 2024; 5: 601-624.
[27] Wang K, Luo L, Fu S, Wang M, Wang Z, Dong L, Wu X, Dai L, Peng Y, Shen G, Chen HN, Nice EC, Wei X and Huang C. PHGDH arginine methylation by PRMT1 promotes serine synthesis and represents a therapeutic vulnerability in hepatocellular carcinoma. Nat Commun 2023; 14: 1011.
[28] Shi Y, Niu Y, Yuan Y, Li K, Zhong C, Qiu Z, Li K, Lin Z, Yang Z, Zuo D, Qiu J, He W, Wang C, Liao Y, Wang G, Yuan Y and Li B. PRMT3-mediated arginine methylation of IGF2BP1 promotes oxaliplatin resistance in liver cancer. Nat Commun 2023; 14: 1932.
[29] Xie F, Zhang H, Zhu K, Jiang CS, Zhang X, Chang H, Qiao Y, Sun M, Wang J, Wang M, Tan J, Wang T, Zhao L, Zhang Y, Lin J, Zhang C, Liu S, Zhao J, Luo C, Zhang S and Shan C. PRMT5 promotes ovarian cancer growth through enhancing Warburg effect by methylating ENO1. MedComm (2020) 2023; 4: e245.
[30] Wu Y, Wang Z, Han L, Guo Z, Yan B, Guo L, Zhao H, Wei M, Hou N, Ye J, Wang Z, Shi C, Liu S, Chen C, Chen S, Wang T, Yi J, Zhou J, Yao L, Zhou W, Ling R and Zhang J. PRMT5 regulates RNA m6A demethylation for doxorubicin sensitivity in breast cancer. Mol Ther 2022; 30: 2603-2617.
[31] Kim H, Kim H, Feng Y, Li Y, Tamiya H, Tocci S and Ronai ZA. PRMT5 control of cGAS/STING and NLRC5 pathways defines melanoma re-

sponse to antitumor immunity. Sci Transl Med 2020; 12: eaaz5683.
[32] Zhu J, Wu Y, Yu Y, Li Y, Shen J and Zhang R. MYBL1 induces transcriptional activation of ANGPT2 to promote tumor angiogenesis and confer sorafenib resistance in human hepatocellular carcinoma. Cell Death Dis 2022; 13: 727.
[33] Engstrom LD, Aranda R, Waters L, Moya K, Bowcut V, Vegar L, Trinh D, Hebbert A, Smith CR, Kulyk S, Lawson JD, He L, Hover LD, Fernandez-Banet J, Hallin J, Vanderpool D, Briere DM, Blaj A, Marx MA, Rodon J, Offin M, Arbour KC, Johnson ML, Kwiatkowski DJ, Janne PA, Haddox CL, Papadopoulos KP, Henry JT, Leventakos K, Christensen JG, Shazer R and Olson P. MRTX1719 is an MTA-cooperative PRMT5 inhibitor that exhibits synthetic lethality in preclinical models and patients with MTAP-deleted cancer. Cancer Discov 2023; 13: 2412-2431.
[34] Cao X, Geng Q, Fan D, Wang Q, Wang X, Zhang M, Zhao L, Jiao Y, Deng T, Liu H, Zhou J, Jia L and Xiao C. m(6)A methylation: a process reshaping the tumour immune microenvironment and regulating immune evasion. Mol Cancer 2023; 22: 42.
[35] Wang Y, Wang Y, Patel H, Chen J, Wang J, Chen ZS and Wang H. Epigenetic modification of m(6)A regulator proteins in cancer. Mol Cancer 2023; 22: 102.
[36] Zhao Z, Yang L, Fang S, Zheng L, Wu F, Chen W, Song J, Chen M and Ji J. The effect of m6A methylation regulatory factors on the malignant progression and clinical prognosis of hepatocellular carcinoma. Front Oncol 2020; 10: 1435.
[37] Cai X, Chen Y, Man D, Yang B, Feng X, Zhang D, Chen J and Wu J. RBM15 promotes hepatocellular carcinoma progression by regulating N6-methyladenosine modification of YES1 mRNA in an IGF2BP1-dependent manner. Cell Death Discov 2021; 7: 315.
[38] Barre-Villeneuve C, Laudie M, Carpentier MC, Kuhn L, Lagrange T and Azevedo-Favory J. The unique dual targeting of AGO1 by two types of PRMT enzymes promotes phasiRNA loading in Arabidopsis thaliana. Nucleic Acids Res 2024; 52: 2480-2497.
[39] Park SH, Ju JS, Woo H, Yun HJ, Lee SB, Kim SH, Gyorffy B, Kim EJ, Kim H, Han HD, Eyun SI, Lee JH and Park YY. The m(6)A writer RBM15 drives the growth of triple-negative breast cancer cells through the stimulation of serine and glycine metabolism. Exp Mol Med 2024; 56: 1373-1387.
[40] Feng J, Li Y, He F and Zhang F. RBM15 silencing promotes ferroptosis by regulating the TGF-beta/Smad2 pathway in lung cancer. Environ Toxicol 2023; 38: 950-961.
[41] Zhao Y, Yan X, Wang Y, Zhou J and Yu Y. N6-methyladenosine regulators promote malignant progression of gastric adenocarcinoma. Front Oncol 2022; 11: 726018.
[42] Yu J, Li W, Hou GJ, Sun DP, Yang Y, Yuan SX, Dai ZH, Yin HZ, Sun SH, Huang G, Zhou WP and Yang F. Circular RNA cFAM210A, degradable by HBx, inhibits HCC tumorigenesis by suppressing YBX1 transactivation. Exp Mol Med 2023; 55: 2390-2401.
[43] Wang X, Tian L, Li Y, Wang J, Yan B, Yang L, Li Q, Zhao R, Liu M, Wang P and Sun Y. RBM15 facilitates laryngeal squamous cell carcinoma progression by regulating TMBIM6 stability through IGF2BP3 dependent. J Exp Clin Cancer Res 2021; 40: 80.
[44] Kang N, Son S, Min S, Hong H, Kim C, An J, Kim JS and Kang H. Stimuli-responsive ferroptosis for cancer therapy. Chem Soc Rev 2023; 52: 3955-3972.
[45] Lei G, Zhuang L and Gan B. Targeting ferroptosis as a vulnerability in cancer. Nat Rev Cancer 2022; 22: 381-396.
[46] Park MW, Cha HW, Kim J, Kim JH, Yang H, Yoon S, Boonpraman N, Yi SS, Yoo ID and Moon JS. NOX4 promotes ferroptosis of astrocytes by oxidative stress-induced lipid peroxidation via the impairment of mitochondrial metabolism in Alzheimer's diseases. Redox Biol 2021; 41: 101947.
[47] Wei S, Qiu T, Yao X, Wang N, Jiang L, Jia X, Tao Y, Wang Z, Pei P, Zhang J, Zhu Y, Yang G, Liu X, Liu S and Sun X. Arsenic induces pancreatic dysfunction and ferroptosis via mitochondrial ROS-autophagy-lysosomal pathway. J Hazard Mater 2020; 384: 121390.
[48] Pan C, Banerjee K, Lehmann GL, Almeida D, Hajjar KA, Benedicto I, Jiang Z, Radu RA, Thompson DH, Rodriguez-Boulan E and Nociari MM. Lipofuscin causes atypical necroptosis through lysosomal membrane permeabilization. Proc Natl Acad Sci U S A 2021; 118: e2100122118.
[49] Yu M, Yu J, Yi Y, Chen T, Yu L, Zeng W, Ouyang XK, Huang C, Sun S, Wang Y, Liu Y, Lin C, Wu M and Mei L. Oxidative stress-amplified nanomedicine for intensified ferroptosis-apoptosis combined tumor therapy. J Control Release 2022; 347: 104-114.
[50] Gao W, Wang X, Zhou Y, Wang X and Yu Y. Autophagy, ferroptosis, pyroptosis, and necroptosis in tumor immunotherapy. Signal Transduct Target Ther 2022; 7: 196.
[51] Wang P, Yao Q, Zhu D, Yang X, Chen Q, Lu Q and Liu A. Resveratrol protects against deoxynivalenol-induced ferroptosis in HepG2 cells. Toxicology 2023; 494: 153589.